

Transport and fluorescence emission properties of photoresponsive ligands

P S ZACHARIAS* and S AMEERUNISHA

School of Chemistry, University of Hyderabad, Hyderabad 500 046, India
e-mail: pszsc@uohyd.ernet.in

Abstract. New photoresponsive azobenzene systems L^1 – L^{10} have been synthesised and characterised. On irradiation at ~ 330 nm, they undergo conversion from *E* to *Z* form to a varying extent, depending on the nature and position of substitution on the azobenzene rings. They revert to *E* form in the dark. Photochemical equilibria have been studied in acetonitrile, *o*-dichlorobenzene and DMF. *E* forms are stabilized more in *o*-dichlorobenzene than in acetonitrile. Two of the molecules L^1 and L^5 show enhanced transport of Cu^{2+} ions across liquid membrane on irradiation. Compounds L^2 and L^3 undergo *E* \rightarrow *Z* photoisomerisation on irradiation at ~ 330 nm accompanied by fluorescence enhancement. *Z* \rightarrow *E* isomerisation in the dark is accompanied by decrease in the fluorescence intensity. These are the first reported examples of fluorescence enhancement on *E* \rightarrow *Z* isomerisation across N=N bond. Protonation of azo groups in L^2 and L^3 is accompanied by fluorescence enhancement. The origin of the fluorescence enhancement in the *cis* isomer is explained on the basis of the inhibition of photoinduced electron transfer due to the nonplanar geometry of this isomer which reduces the effective conjugation of the nitrogen lone pair electrons with the π electrons of the fluorophore.

Keywords. Photoresponsive systems; isomerisation; transport; fluorescence.

1. Introduction

The design of molecular systems which change their physical and chemical properties in response to light is of interest because of a wide range of applications^{1–4}. Azobenzene and its derivatives undergo conversion from the *trans E* form to the *cis Z* form on irradiation at 310 nm and reverts to the *E* form on irradiation at 440 nm or in the dark. This photochemical switching leads to a photostationary equilibrium (PSE)⁵. Shinkai established the *cis-trans* isomerisation of azobenzene as a tool to change the ion extractability of crown ether family, to monitor the rate of conformational changes of crown ethers and polymers and to enforce a change in the conformation of macromolecules in solution⁶. Azo *bis* crown ethers⁷ and several acyclic azobenzene derivatives⁸ which adopt face-to-face orientation enhances the binding abilities of large alkali metal cations and transition metal ions.

Cations are known to be transported through membranes by photoresponsive carriers. The light driven ion transport is attributed to the enhanced binding ability of the *Z* form to extract ions from the source phase and transport them to the receiving phase. At the receiving interface, the irradiation is changed so as to isomerise the *Z* form to the *E* form.

*For correspondence

This initiates decomplexation thereby enriching the receiving phase with the transported ions. The most efficient light driven ion transport is possible for moderately stable complexes.

Supramolecular receptors for fluorescence sensing was first described by Sousa and Larson in 1977⁹. Naphthalene outfitted with crown ether binding site can monitor the association of alkaline earth metals from the changes in the naphthalene fluorescence. Since then, fluorescent chemosensors have been developed by several groups^{10,11}. Reversible *trans-cis* isomerisation of azobenzene derivatives generally does not induce fluorescence effect since azo compounds do not emit¹³. However on suitable coupling of fluorophores like 1-aminonaphthalene and 2-aminobenzoic acid to azobenzene systems, the *trans* \leftrightarrow *cis* isomerisation of the system induces changes in the fluorescence properties of the fluorophores.

Since most of the reported photoresponsive systems contain large macrocyclic systems, it is of interest to examine the possibility of photoinduced *E* \leftrightarrow *Z* isomerisation and metal ion transport involving simple acyclic molecular systems. In this paper, synthesis of photoresponsive aldehydes and Schiff bases, photoinduced metal ion transport by some of these molecules across an organic liquid membrane and fluorescence changes in azo benzene systems due to *trans* \leftrightarrow *cis* isomerisation are discussed.

2. Experimental

2.1 Synthesis of 4,9-dioxo-3,10-dioxa-6,7-diaza-2,11(1,2)5,8(1,4)-tetrabenzena dodecaphan-6-ene-1,12-dial (*L*¹)

Salicylaldehyde (2 mM) was stirred with triethylamine (1 cm³) in toluene (100 cm³) under nitrogen at room temperature for 30 min. Then 4,4'-bis(chlorocarbonyl) azobenzene (1 mM) in toluene (100 cm³) was added dropwise under nitrogen and stirred for 24 h at room temperature. The bulk precipitate was filtered, washed repeatedly with water and toluene, dried and recrystallized from hot toluene, as light pink needles.

2.2 Synthesis of Schiff bases (*L*²-*L*⁵)

Compound *L*¹ (1 mM) in toluene (30 cm³) was heated under reflux with 1-amino naphthalene or 2-aminobenzoic acid or 2-aminophenol or 3-aminopyridine (2 mM) in toluene (30 cm³) under nitrogen for 24 h. The solution was filtered and the volume of the filtrate was reduced to give compounds *L*²-*L*⁵. They were recrystallized from chloroform.

2.3 Synthesis of 4,9-dioxo-3,10-dioxa-6,7-diaza-2,5,8,11(1,4)-tetrabenzena dodecaphan-6-ene-1,12-dial (*L*⁶)

4-hydroxy benzaldehyde (2 mM) was stirred with triethylamine (1 cm³) in toluene (100 cm³) under nitrogen at room temperature for 30 min. Then 4,4'-bis(chlorocarbonyl) azobenzene (1 mM) in toluene (100 cm³) was added dropwise under nitrogen and stirred for 24 h at room temperature. The bulk precipitate obtained was filtered, washed repeatedly with water and toluene, dried and recrystallized from hot toluene, as light pink needles.

2.4 Synthesis of Schiff bases (L^7 – L^9)

Compound L^6 (1 mM) in toluene (30 cm³) was heated under reflux with 2-aminobenzoic acid or 2-aminophenol or 3-aminopyridine (2 mM) in toluene (30 cm³) under nitrogen for 24 h. The precipitate was filtered, washed with hot toluene and recrystallized from chloroform to give compounds L^7 , L^8 and L^9 .

2.5 Synthesis of (2³,2⁵,11²,11⁶)-tetraformyl-3,10-dioxo-6,7-diaza-2,5,8,11(1,4)-tetra-benzenadodecaphan-6-ene-4,9-dione (L^{10})

2-Hydroxy-5-methylbenzene-1,3-dicarbaldehyde (2 mM) in toluene (100 cm³) was stirred with triethylamine (1 cm³) at room temperature for 30 min. To this, 4,4'-bis(chlorocarbonyl)azobenzene (1 mM) was added dropwise under nitrogen. After the addition, the reaction mixture was heated under reflux for 24 h and cooled. The precipitate was filtered, washed thoroughly with water and toluene and recrystallized from chloroform.

2.6 Synthesis of molecule L^{11} and L^{12}

Salicylaldehyde (1 mmol) was stirred with 1 ml of triethylamine in 60 ml toluene under nitrogen at room temperature for ½ h. Then 1 mmol of benzoyl chloride in 60 ml of toluene was added dropwise under nitrogen, stirred for 24 h at room temperature. The white precipitate of triethylamine hydrochloride was filtered off and the volume of the filtrate was reduced to give a light yellow oil which was washed with water and dried over anhydrous MgSO₄. This compound (1 mmol) in 60 ml toluene was heated under reflux with 1 mmol of 1-amino naphthalene or *o*-amino benzoic acid for 24 h and cooled. Evaporation of toluene gave the compounds L^{11} and L^{12} which were characterized by IR and ¹H NMR data. The ligands L^1 – L^{12} are shown in figure 1.

2.7 Photoisomerisation and kinetic measurements

Photoisomerisation of *E* to *Z* form was carried out in *o*-dichloro benzene with a 150W xenon short arc lamp provided with an *f*/4 monochromator. The distance from the source was maintained at 45 cm. The absorbance was recorded at room temperature in the range 600–275 nm in *o*-dichlorobenzene. Subsequently the samples were irradiated at 330 nm and the absorbance of the band was monitored as a function of time. Irradiation was discontinued when the photostationary equilibrium (PSE) was reached (when no further change in ϵ values of the band occurred). When the PSE was reached, the sample was quickly transferred to a standard measuring flask and kept in the dark to carry out the kinetic measurements. The absorbance of the band at 330 nm was recorded as a function of time in the dark. The percentage compositions of *Z* and *E* isomers were calculated on the assumption that the *E* isomer is 100% before irradiation.

2.8 Photoinduced transport experiments

Photoinduced transport of Cu²⁺ ions by molecules (L^1 – L^{10}) across an *o*-dichloro benzene membrane was carried out in a mini U-tube of 3 mm diameter, 50 mm height and base width of 8 mm at 27°C. The source phase contained 1×10^{-3} mol dm⁻³ of Cu(ClO₄)₂·6H₂O in water (75 μ L) (1 μ L = 1 mm³), the membrane phase contained

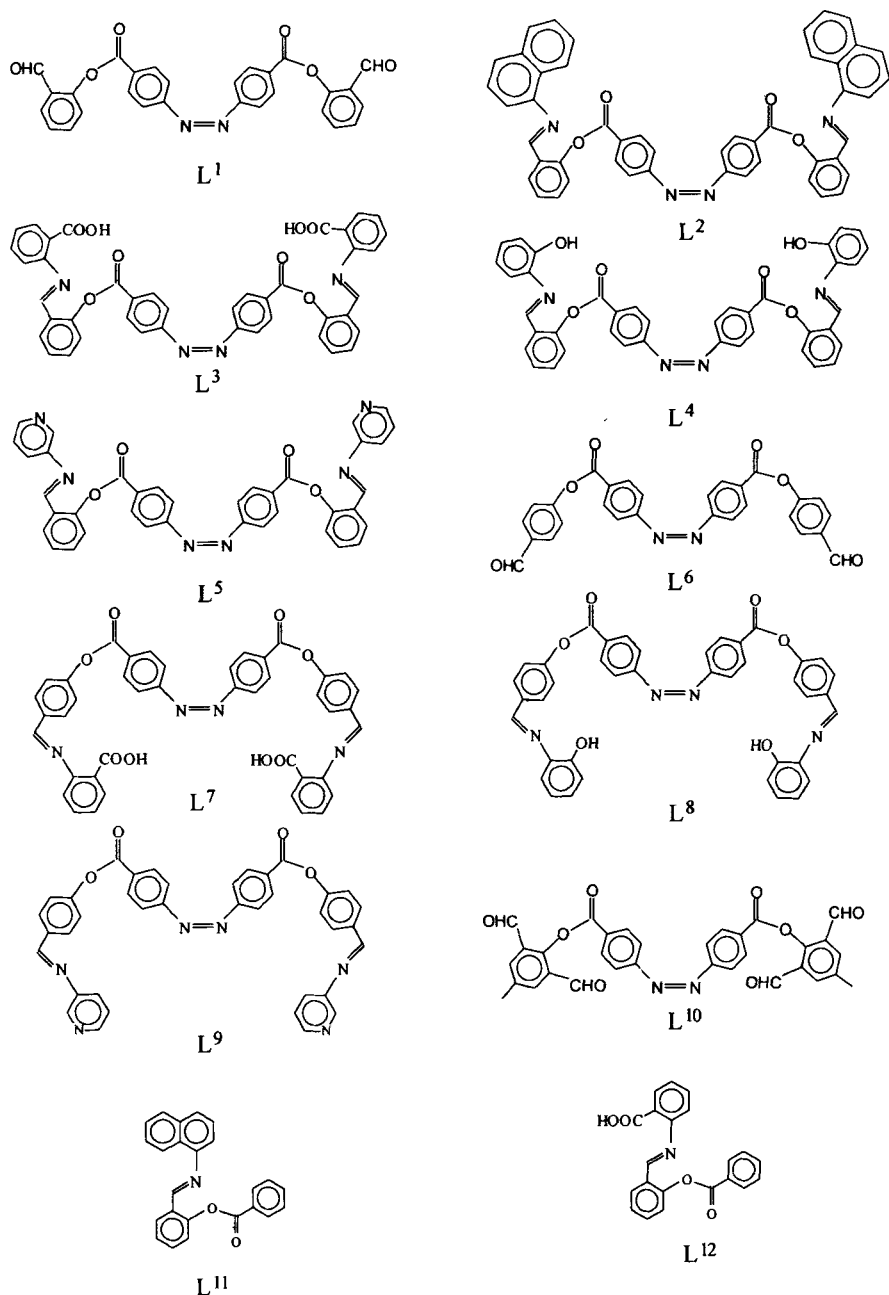


Figure 1. Structures of the ligands L¹–L¹².

0.5×10^{-3} mol dm⁻³ of carrier in *o*-dichloro benzene (0.1 cm³) and the receiving phase contained pure distilled water (75 μ L). The membrane phase was irradiated for 1 h at intervals of 24 h with an *f*/4 monochromator at 330 nm. The distance from the lamp was

maintained at 45 cm. After irradiation, the U-tubes were thermostatted to 27°C and kept in the dark. A sample of the receiving phase (30 μL) was withdrawn after 72 h, and analysed for the presence of Cu^{2+} ions by the carbamate method. Similar experiments were conducted without irradiation and in the absence of carrier molecules to determine the effect of irradiation on the transport of ions and the membrane phase leakage respectively.

2.9 Fluorescence experiments

The concentration of the samples was maintained at $\sim 0.25 \times 10^{-4}$ M. The fluorescence spectra were recorded before irradiation and subsequently the samples were irradiated at ~ 330 nm and fluorescence emission at ~ 400 nm was recorded as a function of time. Both emission and excitation slit band widths (EmSBW and ExSBW) were 5 nm in all the cases. After the attainment of PSE, irradiation was discontinued and the fluorescence spectra for the backward $Z \rightarrow E$ reactions were recorded as a function of time in the dark. Quantum yields were calculated by the comparison of the areas under the curves of isoptical density solutions of samples and quinine sulphate ($\sim 1 \times 10^{-4}$ M concentration in 1N H_2SO_4). Effect of concentration of protons on the emission spectra was studied by adding different concentrations of ~ 0.1 M H_2SO_4 to isoptical density solutions of L^2 and L^3 (optical density was 0.6 at $\lambda = 330$ nm).

2.10 Excited state lifetime measurements

Excited state lifetime measurements were done on IBH 5000 single photon counting spectrofluorometer. The source was a H_2 discharge coaxial nanosecond flash lamp with a pulse width of 1.4 ns and the photomultiplier was Hamamatsu 3235. One thousand counts were employed in all the cases. The fluorescence decay of all the samples studied were fitted to biexponential decay function which yielded better χ^2 values (1.435). Deconvolution was carried out by the method of iterative reconvolution of the instrument response function and the assumed decay function. The goodness of the fit of the experimental data to the assumed decay function was judged by the standard statistical tests (i.e.) random distribution of weighted residuals, the auto correlation function and the values of reduced χ^2 . The estimated error limit on the relative amplitudes is less than 2%–3%.

3. Results and discussion

The molecules L^1 – L^{10} were characterised by CHN, IR and ^1H NMR data. Doublets around 8.38 δ and 8.12 δ in all the systems due to protons on the azobenzene rings, singlets around 10.2 δ in L^1 , L^6 and L^{10} due to aldehydic protons and a singlet around 8.6 δ in Schiff bases due to the azomethine group ($-\text{CH}=\text{N}-$) are identified. Absence of aldehydic peak in Schiff bases confirms that Schiff base condensation is complete.

UV-VIS absorption spectra

The UV-VIS spectral data of these molecules are listed in table 1. The absorbance band at ≈ 330 nm is related to the $\pi-\pi^*$ transition of the $\text{N}=\text{N}$ unit and is a measure of the composition of the E form. It is assumed that the percentage composition of the Z form is negligible compared to that of the E form under normal conditions. The low intensity

Table 1. UV-VIS spectral data of ligands L¹-L¹⁰.

Molecule	Solvent	Before irradiation $\lambda(\epsilon)$	After irradiation $\lambda(\epsilon)$	Z:E
L ¹	MeCN	458(1100)	441(1705)	47:53
		328(50300)	327(26175)	
	1,2-Cl ₂ -C ₆ H ₄	467(1300)	467(1600)	12:88
L ²	1,2-Cl ₂ -C ₆ H ₄	335(51600)	336(45300)	14:86
		455(1630)	449(1300)	
		335(34800)	335(30100)	
L ³	1,2-Cl ₂ -C ₆ H ₄	460(750)	460(900)	27:73
		330(40900)	330(29750)	
L ⁴	MeCN	402(2550)	402(2580)	13:87
		330(23500)	330(20100)	
	1,2-Cl ₂ -C ₆ H ₄	431(1670)	431(1970)	46:54
L ⁵	MeCN	336(63900)	336(34500)	7:93
		461(750)	447(920)	
	1,2-Cl ₂ -C ₆ H ₄	326(41700)	328(33300)	5:95
L ⁶	MeCN	460(752)	461(842)	5:95
		339(54454)	339(51522)	
	1,2-Cl ₂ -C ₆ H ₄	459(500)	451(800)	51:49
L ⁷	DMF	327(21200)	328(10500)	12:88
		467(1070)	467(1580)	
		334(48200)	334(42250)	
L ⁸	DMF	457(750)	457(950)	32:68
		333(42200)	333(28900)	
L ⁹	DMF	452(900)	452(1030)	30:70
		336(48900)	336(29700)	
	MeCN	460(530)	460(650)	32:68
L ¹⁰	MeCN	327(16500)	327(99300)	15:85
		461(550)	461(630)	
	1,2-Cl ₂ -C ₆ H ₄	337(38400)	337(29400)	
L ¹⁰	MeCN	331(6912)	327(1970)	27:73
		323(17622)	328(12850)	

band at ≈ 460 nm is due to the $n-\pi^*$ transition of the N=N unit. Azo compounds undergo $E \rightarrow Z$ isomerisation on irradiation at ~ 330 nm and $Z \rightarrow E$ isomerisation on irradiation at 460 nm or in the dark⁵. During $E \rightarrow Z$ isomerisation the intense absorption band at 330 nm due to the $\pi-\pi^*$ transition of the N=N unit decreases and the absorption maximum of *cis* isomer at 460 nm of the $n-\pi^*$ transition increases. On photoinduced isomerisation, the distance between the para carbon atoms in *trans* azobenzene decreases from about 9.0 Å to 5.5 Å in the *cis* form. Likewise *trans* azobenzene has no dipole moment whereas the nonplanar *cis* compound has dipole moment of 3.0 D¹². *Cis* forms are stabilised more in polar solvents and hence the percentage of this isomer is more in acetonitrile than in *o*-dichloro benzene. The energy difference between the E and Z isomers of azobenzene is found to be 16 kJ/mol from theoretical calculations¹³.

$E \rightarrow Z$ photochemical conversion of compounds L¹-L¹⁰ was determined by measuring the change in absorbance at 330 nm in a 5 min interval during irradiation. The intensity of the $\pi-\pi^*$ transition decreased with irradiation at 330 nm. UV-VIS spectrum of a typical

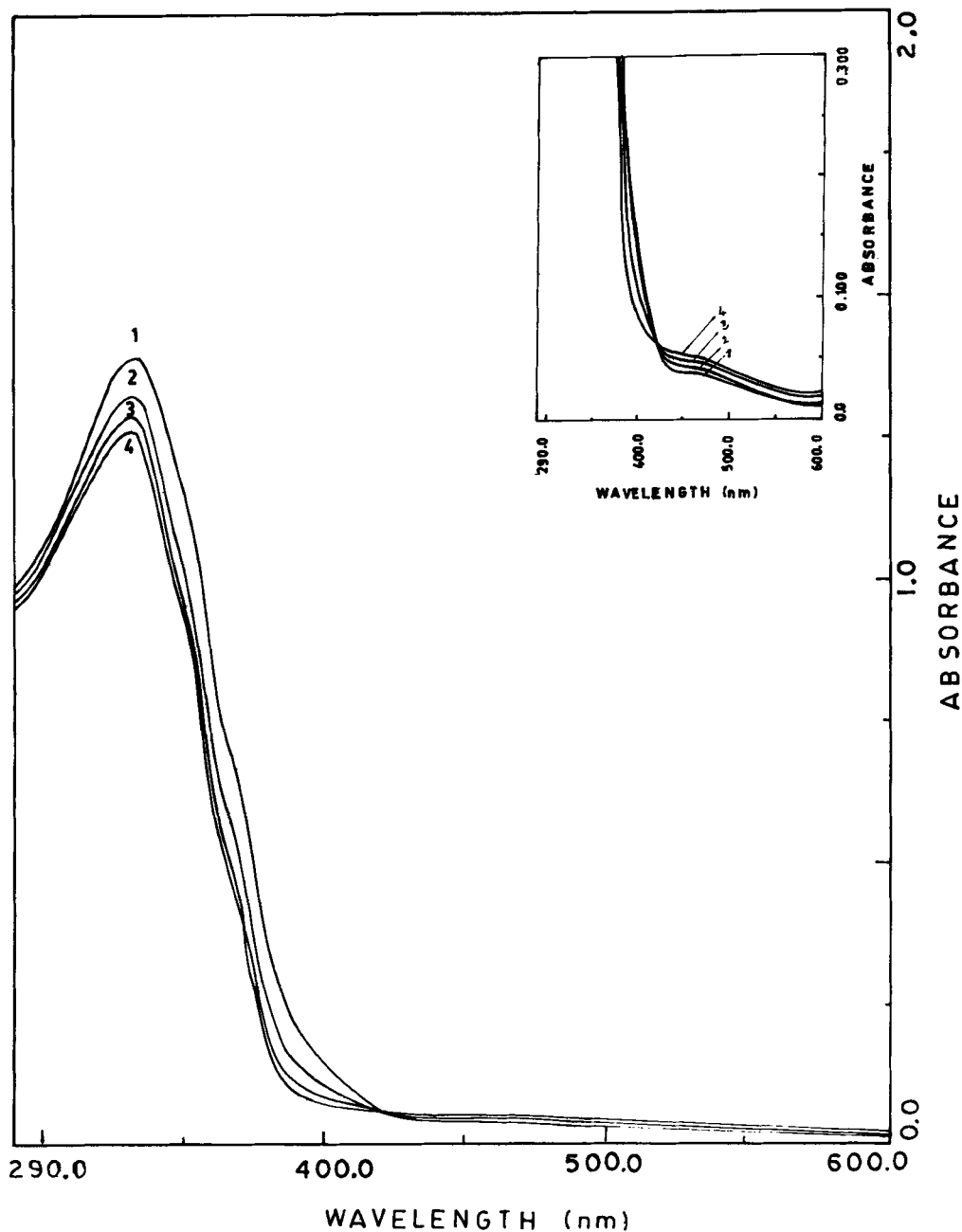


Figure 2. UV-VIS spectra of molecule L^2 and the changes accompanying photochemical conversion of $E \rightarrow Z$ form on irradiation at 335 nm as a function of time; (1) before irradiation; (2) irradiation time 15 min; (3) 30 min; (4) 115 min (inset: increase in the intensity of $n \rightarrow \pi^*$ band as a function of irradiation time).

Schiff base L^2 and the changes accompanying photochemical conversion of $E \rightarrow Z$ forms in *o*-dichloro benzene as a function of irradiation time are presented in figure 2. The UV-VIS spectrum of L^7 in DMF and the changes accompanying the photochemical conversion of $E \rightarrow Z$ forms as a function of irradiation time are presented in figure 3. From UV-VIS spectral measurements it is clear that the band at 330 nm decreases as a function of irradiation time until the photostationary state is reached (i.e. until no further change in the ϵ value of $\pi-\pi^*$ band is observed). The percentage compositions of both the forms at the photostationary state in acetonitrile and *o*-dichlorobenzene as solvents are presented in table 1.

From the data in table 1 it can be seen that a photostationary state is reached faster in *o*-dichlorobenzene than in acetonitrile. The percentage of Z form is lower in *o*-dichlorobenzene than in acetonitrile. The bands due to $\pi-\pi^*$ transitions are shifted to longer wavelengths (red-shifted) in *o*-dichlorobenzene. All these data suggest that the E form is stabilized more in *o*-dichlorobenzene than in acetonitrile. Isomeric composition at the photostationary state depends largely on the nature of the substituents and their positions on the azobenzene ring. The rate constants (k) for the photo and thermal isomerisation processes were determined spectrophotometrically by monitoring the

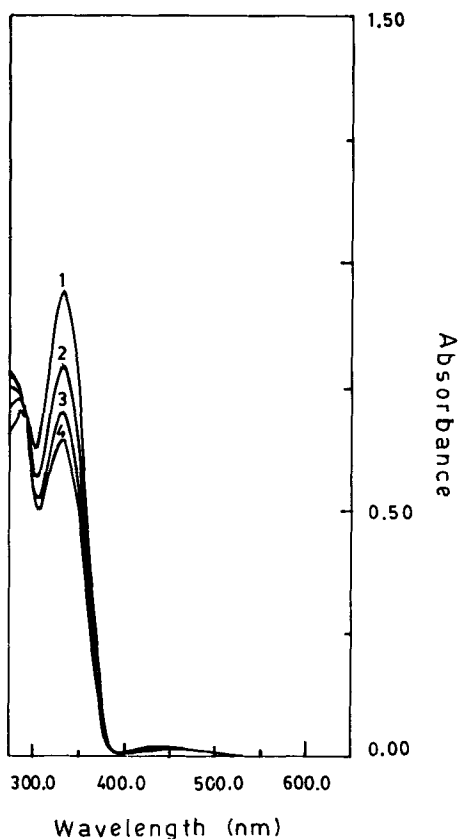


Figure 3. UV-VIS spectra of L^7 and photochemical conversion of $E \rightarrow Z$ form in DMF as a function of time; 1, before irradiation; 2, after irradiation for 10 min; 3, 20 min; 4, 45 min.

decrease in the absorption maxima of the *trans* forms for the forward photoisomerisation process and the increase in the absorption maxima of the *trans* forms for the backward thermal isomerisation process. The rates were found to follow the first order kinetics. The lowest percentage of *Z* form for molecule L⁵ compared to the other molecules may result from the destabilizing steric interactions in the *Z* form. The photoisomerisation rate constant k_{E-Z} is also low. The *E* form was regenerated in less than 2 min in *o*-dichlorobenzene and in about 40 min in acetonitrile for this molecule.

Cu²⁺ ion transport

Of the various strategies adopted to increase the rate of ion transport through membranes, light is one of the most convenient sources though pH and cation concentration gradients can also control the rate of ion transport^{14,15}. Since the molecules L¹–L¹⁰ show varying extent of photoisomerisation to the *Z*-form, photoinduced transport of Cu²⁺ ions by these molecules upon irradiation at 330 nm has been investigated. Photoinduced transport experiments were done as described in the experimental section. Aminolysis of ester groups of carrier ligands is not observed under the present conditions of transport experiments since the carriers were isolated from the membrane phase after 96 h in blank experiments. The IR spectra and the UV-VIS spectra of carriers were found to be unaffected by the contact of distilled water at the interfaces. In the absence of irradiation, the degree of Cu²⁺ ion transport is approximately 20% for the molecules except for L⁵ and L⁹ which is 30%. Irradiation enhances the Cu²⁺ ion transport to 60% for molecule L¹ and about 80% for molecule L⁵. Other molecules do not show any enhanced transport under irradiation conditions. The transport data are given in table 2. The photoinduced ion transport is attributed to the enhanced binding ability of the *Z* forms which extracts ions from the source phase to the liquid membrane phase. This is illustrated in figure 4.

Molecules L⁵ and L⁹ are structurally analogous with a difference only in the position of substitution. In molecule L⁵, the pyridinyl group is substituted at the *ortho* position of the azobenzene derivative, whereas in molecule L⁹, this substitution is at the *para* position. The large increase in the transport of Cu²⁺ ions by molecule L⁵ on irradiation

Table 2. Cu²⁺ ion transport data for carrier molecules L¹–L¹⁰.

Molecule	% Cu ²⁺ in RP with irradiation ^a	% Cu ²⁺ in RP without irradiation ^a
L ¹	62	21
L ²	^b	^b
L ³	33	33
L ⁴	12	5.7
L ⁵	82	32
L ⁶	20	16
L ⁷	^b	^b
L ⁸	^b	^b
L ⁹	32	30
L ¹⁰	19	32

^aOrganic phase (0.1 cm³), carriers (L¹–L¹⁰) = 0.5 × 10⁻³ mol dm⁻³ in *o*-dichlorobenzene; SP (75 μL), [Cu(ClO₄)₂·6H₂O] = 1 × 10⁻³ mol dm⁻³; RP (75 μL), distilled water. After 72 h

^bNot done; due to the insolubility of the compounds L⁷ and L⁸ in *o*-dichlorobenzene

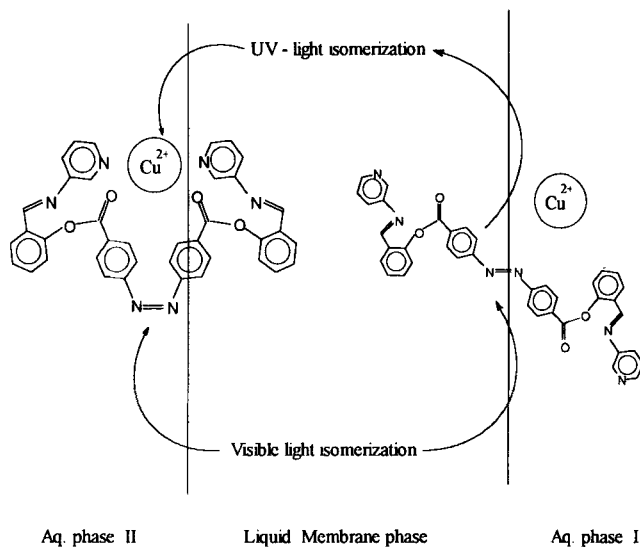


Figure 4. Schematic representation of ion transport accelerated by photoinduced isomerization of L^5 .

indicates that the pyridinyl group, being at the *ortho* position in molecule L^5 , may assist complex formation through the pyridine nitrogen in the *Z* isomer. This additional stabilization appears to be the driving force for the enhanced Cu^{2+} ion transport. For molecule L^9 , the substitution being at the *para* position, does not have similar driving force and hence shows no increase in the transport upon irradiation. A similar explanation is offered to account for the increased Cu^{2+} ion transport by molecule L^1 . The $-CHO$ substitution at the *ortho* position in molecule L^1 compared to molecule L^6 where it is at the *para* position, may facilitate complex formation in the *Z* isomer through oxygen atom participation thereby enhancing the photoinduced Cu^{2+} ion transport. Irradiation does not enhance the transport of Cu^{2+} ions by the molecule L^{10} , which has a total of four $-CHO$ groups at the *ortho* positions of the azobenzene derivative. This may be due to the steric interaction from four aldehydic groups in the *Z* form, reducing the possibility of complex formation and hence transport.

The percentage of Cu^{2+} ion transport is approximately the same (i.e.) $\sim 33\%$ with and without irradiation when molecule L^3 is used as a carrier. This can be contrasted with that of L^5 which is reported to transport 80% of Cu^{2+} ions upon irradiation. Desktop models of the molecules L^3 and L^5 indicate that complexation is favoured in $E-L^3$ whereas L^5 can extract ions only in the *Z* configuration. Hence the $E \rightarrow Z$ isomerisation effects transport in the case of L^5 .

Fluorescence emission spectra

The high intensity band at ~ 330 nm of the UV-VIS spectra of the fluorophore containing ligands L^2 and L^3 was excited and monomer-like emissions were observed at ~ 406 nm for L^2 and at 400 nm for L^3 . The position of $Em\lambda$ showed minor deviations depending on the nature of fluorophore. Emission profiles as a function of irradiation time for molecule L^2

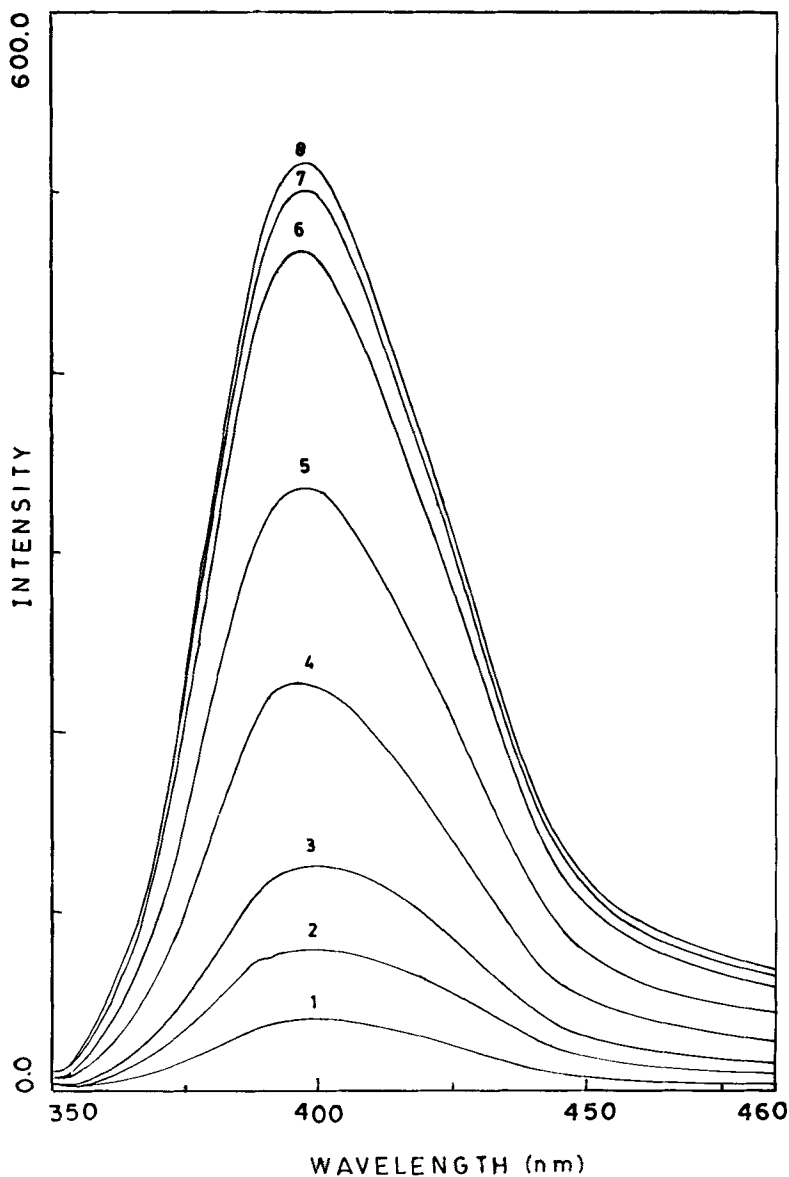


Figure 5. Corrected emission spectra of molecule L^2 as a function of irradiation time for forward $E \rightarrow Z$ process; (1) before irradiation; (2) irradiation time 5 min; (3) 15 min; (4) 30 min; (5) 45 min; (6) 60 min; (7) 75 min; and (8) 115 min.

are shown in figure 5. Emission spectra as a function of time in dark for molecule L^2 are shown in figure 6. Similar trends are observed in L^3 also. Emission spectral data of L^2 and L^3 in *o*-dichlorobenzene are given in table 3. Reference compounds L^{11} – L^{14} do not show fluorescence emission enhancement on irradiation at ~ 330 nm. Fluorescence excitation

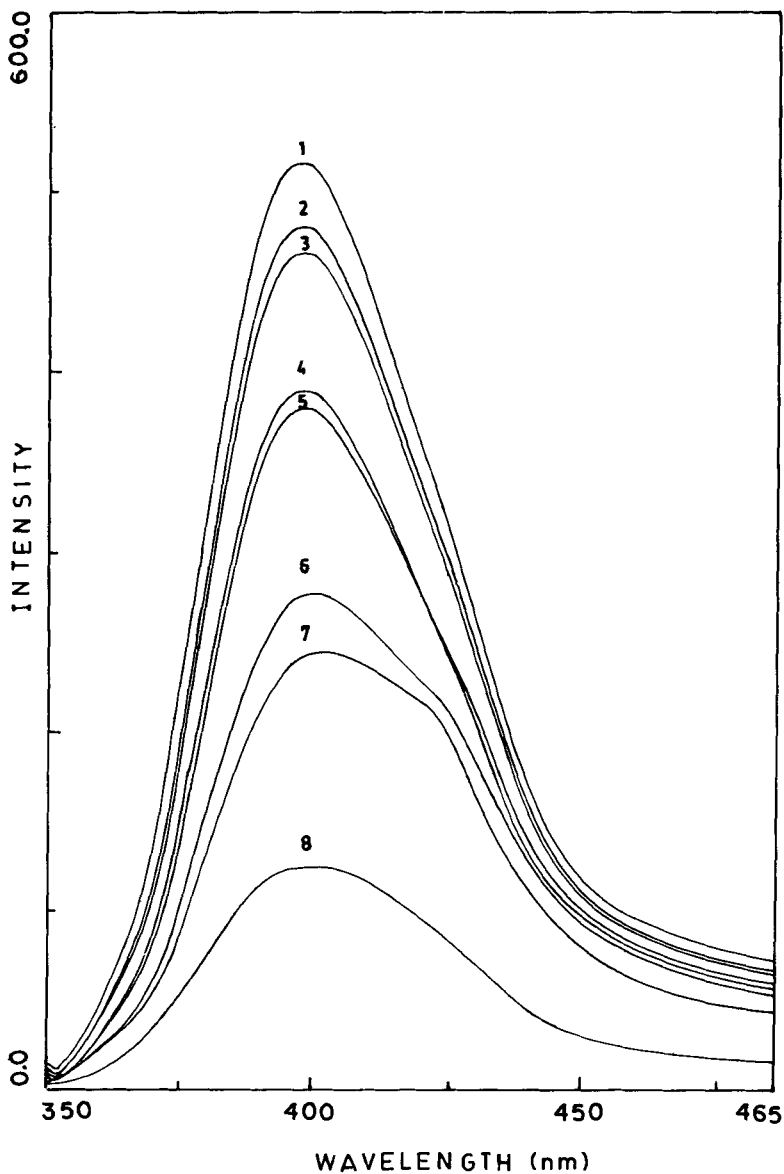


Figure 6. Corrected emission spectra of molecule L^2 as a function of time for backward $Z \rightarrow E$ process in the dark; (1) at the photostationary state; (2) after 4 h in the dark; (3) after 8 h; (4) after 20 h; (5) after 96 h; (6) after 120 h; (7) after 180 h; (8) after 360 h.

spectra have been measured for molecules L^2 and L^3 and they are similar to the UV-VIS absorption spectra in the region 300–385 nm.

These results show that on irradiation, emissions of L^2 and L^3 are enhanced. Generally, azo compounds do not emit even under conditions that normally promote such behaviour. While the emission observed in L^2 and L^3 originate from the fluorophores that are coupled

Table 3. Emission spectral data of molecules L¹, L³, L¹¹ and L¹² in *o*-dichlorobenzene.

Emission ^a	<i>(E) → (Z)</i> ($h\nu$; 335 nm)			<i>(Z) → (E)</i> (dark)		
	ϕ_f	ϕ_z	EF	ϕ_f	t_2 (h)	QF
L ²	0.008	0.104	13	0.026	360	4
L ³	0.110	0.690	6.3	0.266	360	2.6
L ¹¹	0.001	0.001	1.0			
L ¹²	0.390	0.355	^b			

^a ϕ_f → quantum efficiency before irradiation; ϕ_z → quantum efficiency at the photostationary state and ϕ_f → quantum efficiency at the stage of maximum *Z* → *E* conversion in the dark; calculated using quinine sulphate as a standard; t_2 → time required for maximum *Z* → *E* conversion in the dark; EF → enhancement factor, QF → quenching factor

^b Cannot be calculated as the intensity decreased on irradiation

to azobenzene, the enhanced emission of L² and L³ on excitation results from the *E* → *Z* isomerisation already characterised in these systems (vide supra). For the molecule L², the emission was enhanced 13-fold at the photostationary equilibrium (PSE). For L³ emission was enhanced 6-fold of the non-irradiated starting solution at the PSE. There is no further enhancement in emission after the photostationary equilibrium is reached. *Z* → *E* isomerisation in the dark was followed by decrease in the emission intensity. After 360 h in the dark, emission intensity of L² was found to decrease to 3-fold from 13-fold at the photostationary state. In other words, ~ 75% of *Z* → *E* conversion had taken place. In the case of L³, the emission intensity decreased to 2-fold from 6-fold at the photostationary state and the percentage of conversion was found to be ~ 60%.

Additional support to the photo enhanced fluorescence (PEF) of L² and L³ on *E* → *Z* photoisomerisation comes from the following experiments. Molecules L¹¹ and L¹², structurally analogous but without N=N unit were synthesised and the emission spectra were monitored under similar conditions as a function of irradiation time at 330 nm. The emission spectra over a period of 60 min showed only marginal increase in intensity in L¹¹ and marginal decrease in L¹². Similarly the fluorophores, pure 1-aminonaphthalene (L¹³) and *o*-aminobenzoic acid (L¹⁴) were irradiated at ~ 330 nm, and the emission spectra were recorded as a function of irradiation time. In this case too the emission spectra over a period of 60 min showed only marginal variation in intensity in these reference compounds. These results indicate that the enhancement of fluorescence emission in L² and L³ is due to *E* → *Z* isomerisation with respect to -N=N- bond and not due to the isomerisation across the CH=N- bond¹⁶.

The fluorescence enhancement on *cis* isomerisation can be understood as arising from the inhibition of photoinduced electron transfer (PET) mechanism¹⁷. MO theory predicts C_{2h} and C_{2v} symmetry for the n-orbitals of *trans* and *cis* isomers respectively¹³. The *cis* isomer is non-planar and therefore the lone pair electrons on nitrogen can no longer effectively conjugate with π -electrons of the fluorophore thereby inhibiting PET mechanism. The inhibition of PET increases the ϕ_f value of the system (*cis* isomer) to 0.104 from the value of 0.008 (*trans* isomer).

Effect of protonation on emission spectra

Operation of PET phenomenon has been checked by protonation experiments. Titration of L^2 and L^3 with H_2SO_4 , (~ 0.1 M) in DMF leads to the loss of the $n \rightarrow \pi^*$ band at 460 nm in the UV-VIS spectra whereas the $\pi \rightarrow \pi^*$ remained unaffected. Fluorescence was enhanced 3-fold in L^2 and 2.5-fold in L^3 ($Ex\lambda$, 335 nm; $Em\lambda$, 416 nm) at low concentration of protons ($\log [H^+] \sim -1.43$) in DMF. Protonation of $-N=N-$ bond is known at low proton concentration¹⁸. In the protonated form, the lone pair electrons are not available for quenching the fluorescence of fluorophores (electron acceptors) by electron transfer (PET) mechanism and hence enhanced emission can be observed^{17,19}. The enhanced emission follows the order $L^3 > L^2$. The protonation of azo nitrogens also

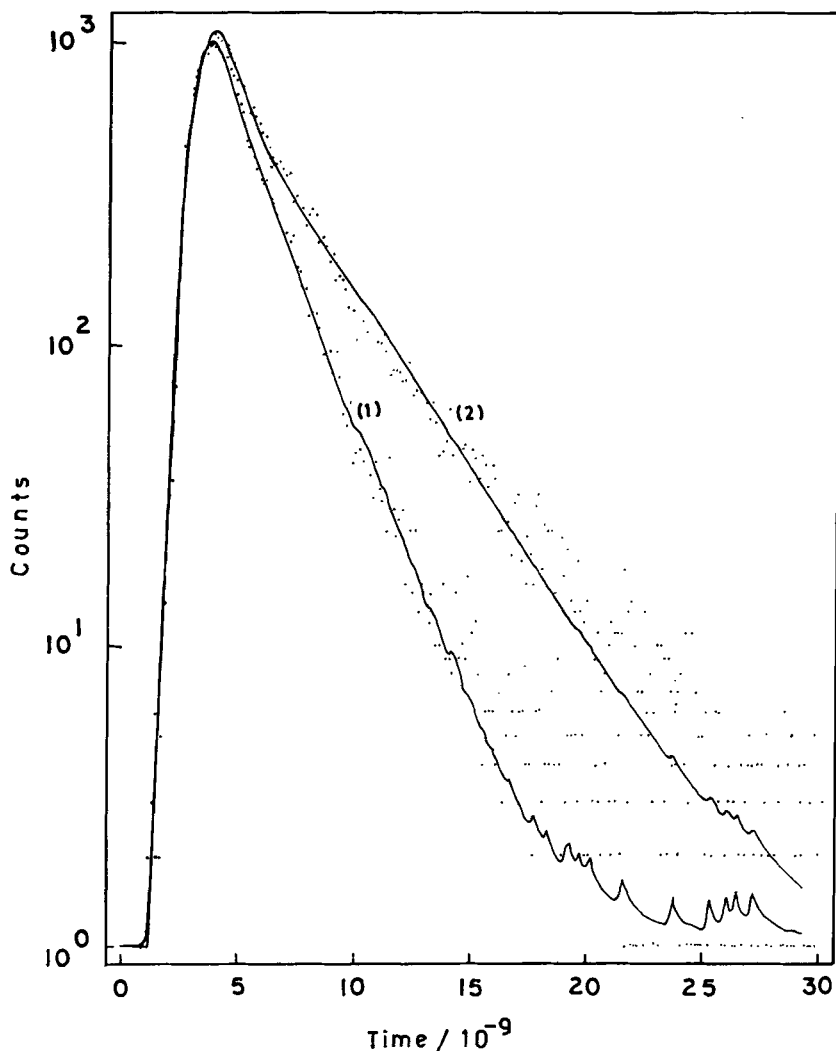


Figure 7. Fluorescence decay pattern of L^2 , (1) before irradiation and (2) after irradiation.

Table 4. Decay parameters of molecules L², L¹¹ and L¹³ in *o*-dichlorobenzene.

Parameters	L ²		L ¹¹		L ¹³	
	Before Irr.	After Irr.	Before Irr.	After Irr.	Before Irr.	After Irr.
τ_{s1}	0.18	0.53	0.65	0.75	0.155	0.171
τ_{s2}	1.9	3.5	3.37	3.9	1.92	1.94
Rel.Amp ₁	84	75.5	85.9	78	92	91
Rel.Amp ₂	16	24.5	14.1	22	08	09
Kr ₁	0.04	0.194	0.0015	0.0024	0.709	0.643
Kr ₂	0.004	0.029	0.0003	0.0004	0.0572	0.0567
Kn _{r1}	5.515	1.692	1.537	1.331	5.74	5.205
Kn _{r2}	0.522	0.256	0.296	0.2566	0.463	0.45876

results in the loss of $n \rightarrow \pi^*$ band at 455 nm in the UV-VIS spectrum. Higher concentration of protons ($\log [H^+] > -0.029$) can lead to the hydrolysis of $-\text{COO}-$ ester groups accompanied by decreased emission intensities by about 2.5-fold in both the cases. This is confirmed by the hydrolysis of L² and L³ which gives the non-fluorescent methyl ester compound in methanol.

In coordinating solvents the ϕ_f values of the *trans* form of L² increases to 0.045 in DMF and 0.036 in MeCN whereas it is 0.008 in *o*-dichloro benzene. Proton transfer from $-\text{COOH}-$ group in L³ to $-\text{N}=\text{N}-$ is also not expected on irradiation. Cleavage of $-\text{CH}=\text{N}-$ bond is insignificant because of the reversibility of the process. The UV-VIS absorption, emission and ¹H NMR spectra remained without any visible changes before and after irradiation except for minor changes in the intensities.

Excited state lifetime measurements of L² before irradiation showed the presence of two kinetically distinguishable species of different amplitudes with shorter lifetimes. On irradiation, the lifetime increases accompanied by changes in the amplitudes of the distinguishable species as shown in figure 7. Photoinduced electron transfer is inhibited on irradiation which increases the lifetime of the excited state. The *cis* isomer of L² has a longer lifetime which is reflected in from figure 7. It is mentioned already that the quenching process, such as photoinduced electron transfer, shortens the lifetime of the excited state⁹. The τ_x values of the reference compounds L¹¹ and L¹³ shown in table 4 remain unaffected by irradiation.

4. Conclusion

These results demonstrate that the molecules (L¹-L¹⁰) undergo $E \leftrightarrow Z$ isomerisation to various extents upon irradiation at 330 nm. Transport of Cu²⁺ ions across a membrane is enhanced only by two systems, L¹ and L⁵ under irradiation conditions. This shows that by proper selection of the substituents on the azobenzene ring, it is possible to enhance photoinduced metal ion transport. It is also demonstrated that $E-Z$ isomerisation across $-\text{N}=\text{N}-$ bond in azobenzene derivatives outfitted with suitable fluorophore can be monitored by fluorescence spectral changes. The isomerisation process is found to be reversible. The fluorescence enhancement is attributed to the inhibition of PET in the *cis* isomer. Protonation of N=N bond results in enhancement of fluorescence emission supporting the operation of PET mechanism.

Acknowledgements

Financial assistance from Council of Scientific and Industrial Research, University Grants Commission and the Department of Science and Technology, New Delhi is gratefully acknowledged.

References

1. Willner I and Willner B 1993 *Bioorganic photochemistry – biological applications of photochemical switches* (ed.) H Morrison (New York: Wiley) 2 1
2. Prasanna de Silva A, Nimal Gunaratne H Q and McCoy C P 1993 *Nature (London)* **364** 42
3. Czarnik A W 1991 *Frontiers in supramolecular chemistry and photochemistry* (eds) H-J Schneider and H Durr (VCH) p. 109
4. Shinkai S and Manabe O 1984 *Top. Curr. Chem.* **121** 67
5. Vogtle F 1993 *Supramolecular chemistry* (New York: Wiley) chap 7
6. Shinkai S, Nakaji T, Nishida Y, Ogawa T and Manabe O 1980 *J. Am. Chem. Soc.* **102** 5860
7. Shinaki S, Yoshida T, Manabe O and Fuchita Y 1988 *J. Chem. Soc., Perkin Trans. I* 1431
8. Blank M, Soo L M, Wassermann N H and Erlanger B F 1981 *Science* **214** 70
9. Sousa L R and Larson J M 1977 *J. Am. Chem. Soc.* **99** 307
10. Czarnik A W 1994 *Acc. Chem. Res.* **27** 302
11. Konopelski J P, Hibert F K, Lehn J-M, Desvergne J-P, Fages F, Castellan A and Laurent H B 1985 *J. Chem. Soc., Chem. Commun.* 433
12. Sudesh Kumar G and Neckers D C 1989 *Chem. Rev.* **89** 1915
13. Rau H 1973 *Angew. Chem. Int. Ed. Engl.* **12** 224
14. Grimaldi J J and Lehn J-M 1979 *J. Am. Chem. Soc.* **101** 1333
15. Sugiura M and Shinbo T 1979 *Bull. Chem. Soc. Jpn.* **52** 684
16. Yan Zhenglin and Wu Shikang 1994 *Wuli Huaxue Xuebao* **10** 610; *Chem. Abstr.* **121** 289365x
17. Bissell R A, Prasanna de Silva A, Nimal Gunaratne H Q, Mark Lynch P L, Maguire G E M, McCoy C P and Sandanayake K R A S 1993 *Top. Curr. Chem.* **168** 223
18. Haselbach E and Heilbronner E 1967 *Tetrahedron Lett.* **46** 4531
19. Cox G S and Turro N J 1984 *J. Am. Chem. Soc.* **106** 422